Bull. Chem. Soc. Ethiop. **2024**, 38(4), 989-1001.
DOI: https://dx.doi.org/10.4314/bcse.v38i4.14

ISSN 1011-3924
Printed in Ethiopia
Online ISSN 1726-801X

A THEORETICAL STUDY ON A NEW DRUG COMBINES BETWEEN VANADYL SULFATE AND VITAMIN E IN A SINGLE COMPONENT: A NOVEL ANTIOXIDANT MEDICATION IN FEMALE REPRODUCTIVE HEALTH

Amnah Mohammed Alsuhaibani[1], Amal Hassan AlShawi[1], Ahmed Gaber[2*], Sonam Shakya[3*] and Moamen S. Refat[4*]

[1]Department of Physical Sports Sciences, College of Sports Sciences & Physical Activity, Princess Nourah bint Abdulrahman University, P.O. Box 84428, Riyadh 11671, Saudi Arabia
[2]Department of Biology, College of Science, Taif University, P.O. Box 11099, Taif 21944, Saudi Arabia
[3]Department of Chemistry, Faculty of Science, Aligarh Muslim University, Aligarh 202002, India
[4]Department of Chemistry, College of Science, Taif University, P.O. Box 11099, Taif 21944, Saudi Arabia

(Received March 1, 2024; Revised April 3, 2024; Accepted April 9, 2024)

ABSTRACT. This study explores the theoretical properties of a novel complex formed by combining vitamin E (VitE) and vanadyl(II) sulfate. The complex, $[VO(VitE)_2(H_2O)_2]2H_2O$ (Vcom), was synthesized in solid form through a reaction between VitE and $VOSO_4.xH_2O$ in a specific solvent mixture and pH. VitE binds to the vanadyl ion as a single ligand via its deprotonated phenolic oxygen. To characterize the complex, various analytical techniques were employed, including elemental analysis, spectral analysis, conductivity measurements, thermal analysis, X-ray diffraction, and microscopy. Electronic and magnetic properties were also investigated. Theoretical calculations - molecular docking simulations were used to assess the binding affinity of Vcom with two receptors known to interact with vitamin E: α-tocopherol transfer protein (α-TTP) and p105 subunit of nuclear factor NF-kappa-B p105 subunit (NF-κB). The findings revealed a square pyramidal geometry for the Vcom complex. Additionally, Density Functional Theory (DFT) were performed on both VitE and Vcom, focusing on their optimized structures, electrostatic properties, and HOMO-LUMO energy gaps. In summary, this research delves into the theoretical aspects of a newly formed VitE-vanadyl complex, providing insights into its structure, properties, and potential interactions with relevant receptors.

KEY WORDS: New drug, Vanadyl sulfate, Vitamin E, Antioxidant, Female, Reproductive health, DFT

INTRODUCTION

Scientists are looking into vanadium compounds like peroxovanadate and vanadyl complexes as potential cancer treatments [1-7]. Vanadium, a tiny amount naturally present in our cells, plays a surprising role in regulating important cellular processes [8]. Certain vanadium compounds, like bis(ethylmaltolato) oxovanadium(IV) (BEOV) and bis(maltolato) oxovanadium(IV) (BMOV), have shown promise in mimicking effects of insulin, making them potentially beneficial for diabetes management [9-11]. In animal studies, BEOV, BMOV, and other vanadium complexes with food-grade additives like maltol and ethylmaltol, have been effective in controlling diabetes [9, 11, 12]. Usefulness of Vanadium in both cancer and diabetes treatment may stem from its ability to block protein tyrosine phosphatase enzymes [8, 13, 14]. Interestingly, depending on the dose and how it's combined with other molecules, vanadium can act as both a pro-oxidant and an antioxidant [14-17].

*Corresponding authors. E-mail: moamen@tu.edu.sa; a.gaber@tu.edu.sa; sonamshakya08@gmail.com

Vitamin E acts as a powerful shield within cells, neutralizing harmful molecules called reactive oxygen species. Unfortunately, various environmental threats can disrupt the delicate balance of reproduction and pregnancy. These risks range from industrial waste and agricultural runoff to polluted water and spills. Such threats can affect crucial stages like pre-conception, gestation, and development, potentially harming both mother and child. Oxidative stress, a harmful imbalance of antioxidants and damaging molecules, is often linked to various reproductive issues, including endometriosis. While the exact role of oxidative stress in endometriosis remains unclear, studies have found elevated levels of stress markers in affected individuals [18-21].

The present research delves into the theoretical antioxidant properties of a newly designed vanadyl(IV)-vitamin E complex (Vcom) with potential benefits for female reproductive health. Using advanced computer simulations, we analyzed its structure, electronic behavior, and interactions with key molecules. Precise three-dimensional structure of Vcom was determined, a crucial step in understanding how it works. We mapped the distribution of electrical charges within Vcom, revealing its potential for interactions with other molecules. Studying the energy gap between specific molecular orbitals (HOMO and LUMO) revealed insights into Vcom's stability and its potential to transfer electrons, key for antioxidant activity. Additionally, we used computer simulations to compare how our new vitamin E complex (Vcom) and regular vitamin E bind to two important molecules in the body: a transport protein called α-tocopherol transfer protein (α-TTP) and a signaling molecule called nuclear factor kappa B (NF-κB). We did this by virtually docking Vcom and vitamin E into these molecules and analyzing how well they fit. We looked at several factors, like how strong the binding is, how exposed the binding site is to water, and the types of interactions involved (like hydrogen bonds or aromatic interactions). This detailed analysis gave us a clearer picture of how Vcom might work compared to regular vitamin E.

EXPERIMENTAL

Synthesis of vanadyl VitE complex

The Vcom (Figure 1) was previously prepared [22] according to the following method: A solution of $VOSO_4.2H_2O$ (1.0 g, 5 mmol) in bi-distilled water (10 mL) was added dropwise to a stirred solution of Vitamin E (4.30 g, 10 mmol) in ethanol (25 mL). The resulting brown solution was stirred for about 45 min while heating at 50 ºC. After a few minutes, the color of the solution changed to a deep green feature. Addition of ammonia solution (5% w/w) till pH = 8 the greenish black precipitate was formed. It was filtered off, washed with ethanol, and dried under vacuum over $CaCl_2$. The vanadyl(II) solid complex (Vcom) was produced in 2.75 g (63.95%) yield. Microchemical analysis data for C and H were repeated twice as follows; calcd for $C_{58}H_{106}O_9V$/Mwt = 997 g/mol: C, 69.81%; H, 10.63%. Found: C, 69.75%; H, 10.55%.

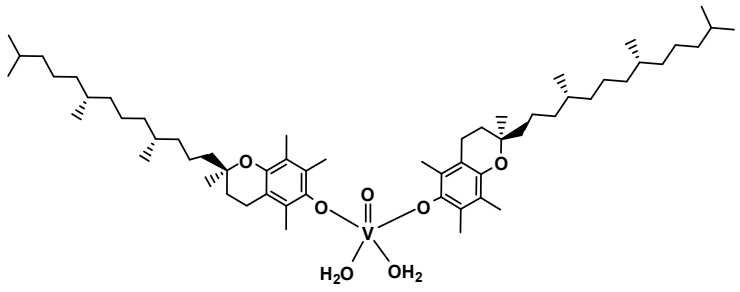

Figure 1. Structure of vanadyl(II) vitamin E complex (Vcom) [22].

DFT and TD-DFT studies

A quantum mechanical modeling technique used in physics and chemistry is called density functional theory (DFT). It finds the electron density distribution and uses that information to evaluate the electronic structure of atoms and molecules. DFT predicts properties like energy, structure, and interactions, making it valuable for studying complex systems in materials science and computational chemistry. We employed the Gaussian 09RevD.01 package [23] for our density functional theory (DFT) studies. These calculations served to attain optimized molecular structures and explore electronic transitions in both VitE and Vcom.

Our theoretical investigation employed the B3LYP/6-311G++ basis set, combining Becke's hybrid exchange function with Pople basis sets and Los Alamos Effective Core Potentials for vanadium [24]. We analyzed crucial properties like electrostatic potential maps, HOMO-LUMO energy gaps, and frontier molecular orbitals (FMOs) for both VitE and Vcom [25]. FMOs provided insights into chemical stability for both the systems. Calculated IR frequencies confirmed optimized structures and vibrational mode analysis enabled accurate FT-IR band assignment. We further calculated structure-based gas-phase molecular properties using the same framework. Visualization was facilitated by ChemCraft 1.5 software [26].

Molecular docking

Molecular docking is a revolutionary tool that helps scientists unlock the secrets of drug-protein interactions, paving the way for faster and more effective drug development. It simulates their binding, predicting the most favorable orientation and conformation. By assessing energetics and geometric complementarity, it estimates the binding affinity. Docking helps identify potential drug candidates, understanding their interactions with protein targets, and aids in the design and optimization of new pharmaceuticals. The entire docking experiment was executed on a processor with the following specifications: Intel(R) Core(TM) i5-4200U CPU @ 1.60 GHz, 2.10 GHz, 2.30 GHz, 64-bit architecture. In this study, the initial molecular structure of VitE and Vcom, which had been optimized through DFT calculations, served as our starting structures. The conversion of these structures into PDBQT format was facilitated by OpenBabelIGUI software, version 2.4.1 [27, 28]. For the receptors, α-TTP (PDB ID: 1OIP) and NF-κB (PDB ID: 1SVC), we retrieved their structural data from the RCSB Protein Data Bank online [29]. The native ligand and any additional heteroatoms, such as water molecules, were then removed from the receptors using BIOVIA Discovery Studio (DS) Visualizer (v19.1.0.18287) to prepare them for the docking process. We used the Autodock Tool [30] to determine the Kollman charges after adding polar hydrogen atoms to the receptor architectures to assure accuracy. The Geistenger method was used to assign partial charges [31]. Using Autodock Vina, the final docking of receptors and ligands (VitE and Vcom) was carried out [31]. Using DS Visualizer (https://www.3ds.com/products-services/biovia/), a thorough study of the docked positions was carried out to evaluate the interactions.

RESULTS AND DISCUSSION

The newly formed greenish-black vanadyl(II) vitamin E complex (Vcom) exhibits non-electrolytic behavior, as inferred from molar conductance measurements [22]. Infrared spectral analysis provides insights into the interaction between vanadyl(II) ions (VO^{2+}) and vitamin E. The $VOSO_4$/vitamin E complex exhibits characteristic bands at 3400, 3160, 3070, and 2800 cm^{-1}, corresponding to the O-H stretching vibrations of bound water molecules. The absence of the typical phenolic group peak suggests a direct bonding interaction between the phenolic oxygen and the vanadyl(II) ion. A new peak at 980 cm^{-1}, attributed to the ν(V=O) stretching mode, confirms the formation of the complex and indicates a square pyramidal geometry around the vanadium center due to the observed frequency shift. A series of measurements, including a

titration curve and analysis of the electronic and magnetic properties, revealed a 1:2, where two vitamin E molecules bind to each vanadyl ion. Further investigation using electronic and magnetic spectroscopy confirmed the square pyramidal structure of the complex, supported by the presence of a characteristic peak at 11,200 cm^{-1} and a magnetic moment of 1.68 BM within the expected range for a specific type of system [22]. Also, electron spin resonance (ESR) spectroscopy $[VO(Vit\ E)_2(H_2O)_2]2H_2O$ complex, measured in a DMSO solution at room temperature, highlights the $g_{\parallel}$, $g_{\perp}$ values that correspond well with a molecule structured in a square pyramidal geometry [22].

X-ray powder diffraction analysis shows the complex doesn't have a repeating crystal structure, suggesting it's like a disordered glass. Heating experiments reveal impressive stability, with no weight loss until temperatures reach 550 °C. At that point, the complex breaks down into vanadium carbide and carbon. Tests against various bacteria show the complex works best against *Bacillus subtilis*, *Streptococcus pneumonia*, and *Escherichia coli*. *Staphylococcus aureus* and *Pseudomonas Sp.* are less affected. Similarly, the complex fights fungus better against *Aspergillus niger* than *Penicillium Sp* [22].

Density functional theory calculations

We utilized the B3LYP:lanL2DZ / 6-311G++ level of theory to obtain optimized structures for both VitE and Vcom. The minimum SCF energy for VitE was calculated to be -1285.372901 atomic units after 20 optimization steps, and for Vcom, it was found to be -2835.359883 atomic units.

Figure 2 shows the ideal structures of both vitamin E and the vanadium complex, revealing their atomic arrangements and relaxed lattice sizes. Figure 3 then reveals the distribution of electrical charges across these molecules by measuring molecular electrostatic potential (MEP) maps. These maps visualize the charge distribution around the molecules, with blue areas representing electron-attracting (electrophilic) regions and red areas representing electron-donating (nucleophilic) regions [32]. By analyzing MEP maps, we can identify potential binding sites for different types of chemical interactions. The color scale used ranges from deep red (highly electronegative) to deep blue (highly electropositive), with vitamin E values between -5.151 and +5.151 e-2 and vanadium complex values between -7.279 and +7.279 e-2 [33].

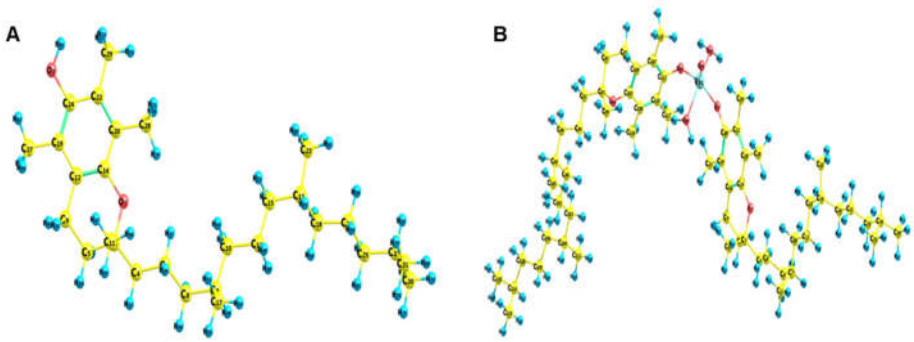

Figure 2. Optimized geometries structure of (a) vitamin E (VitE) only; (b) and vanadyl(II) vitamin E complex (Vcom) with Mulliken atom numbering scheme.

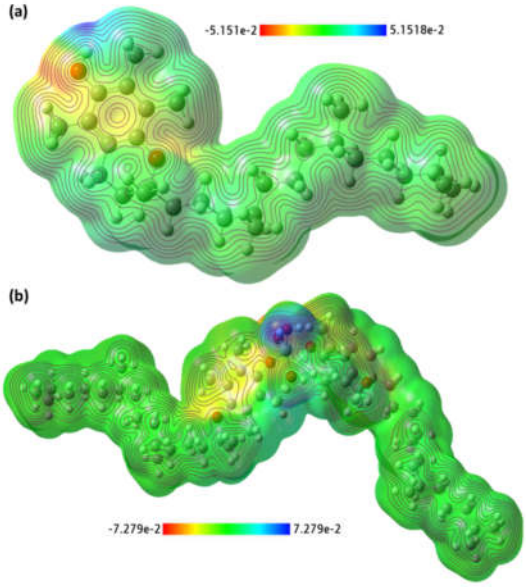

Figure 3. MEP surface map of (a) VitE and (b) synthesized vanadyl(II) vitamin E complex (Vcom) with respective color scales.

We used a computer simulation technique called DFT to predict the infrared (IR) spectra of both vitamin E (VitE) and the vanadyl(II) complex (Vcom) (Figure 4). This allowed us to compare them to the actual IR spectra measured in the lab. Both molecules showed characteristic peaks in their IR "fingerprints," revealing details about their structure and bonding [34]. The simulated spectra for VitE and Vcom, scaled at 0.9442 and 0.8101, respectively. For Vcom, the simulated IR spectrum showed peaks at specific frequencies, which match the water molecules attached to it (3496, 3319, and 3273 cm^{-1}). The stretching vibration motions of C-H bands for both aromatic and aliphatic are presence at 2885 and 2749 cm^{-1}. The stretching vibration of ν(C=C)is presence at 1427 cm^{-1}, and the characteristic frequency of ν(V=O) band concering the vanadyl ion is existed at 994 cm^{-1} (Figure 4a).Similar results were found for VitE only, with peaks representing O-H (3495 cm^{-1}), C-H (2997-2842 cm^{-1}), C=C (1580 cm^{-1}), and C-O (1230 cm^{-1}) bands. It's important to remember that computer simulations cannot be accurate, so a scaling factor was applied to align the simulated and experimental vibrational frequencies [35].

A computer simulation technique called TD-DFT was used to analyze how light interacts with both Vitamin E (VitE) and the vanadyl(II) complex (Vcom) in their gas forms. This helped us understand how they might absorb light at different wavelengths. For VitE, the simulation predicted two absorption peaks. The first area, at a wavelength of 266 nm, corresponds to the most likely excited state of the molecule, where electrons move from a specific orbital (HOMO) to another (LUMO). The second area, at 217 nm, reflects a less likely excited state with a different electron movement (HOMO-1 to LUMO).

The 266 nm peak corresponds to the most excited state of the molecule, where an electron jumps from a specific energy level (HOMO) to another (LUMO) when it absorbs blue light. The 217 nm peak represents a further excited state, involving a different energy level transition (HOMO-1 to LUMO) when absorbing ultraviolet light. On the other hand, Vcom showed three areas of potential light absorption at 326, 270, and 251 nm. The 326 nm peak is the most excited state of the molecule, just like in VitE (HOMO to LUMO). The 270 nm peak represents the next

excited state (HOMO-1 to LUMO transition), and the 251 nm peak corresponds to an even higher energy level transition [36]. This analysis provides valuable insights into how VitE and Vcom interact with light, which can be crucial for understanding their potential applications in fields like medicine and solar energy.

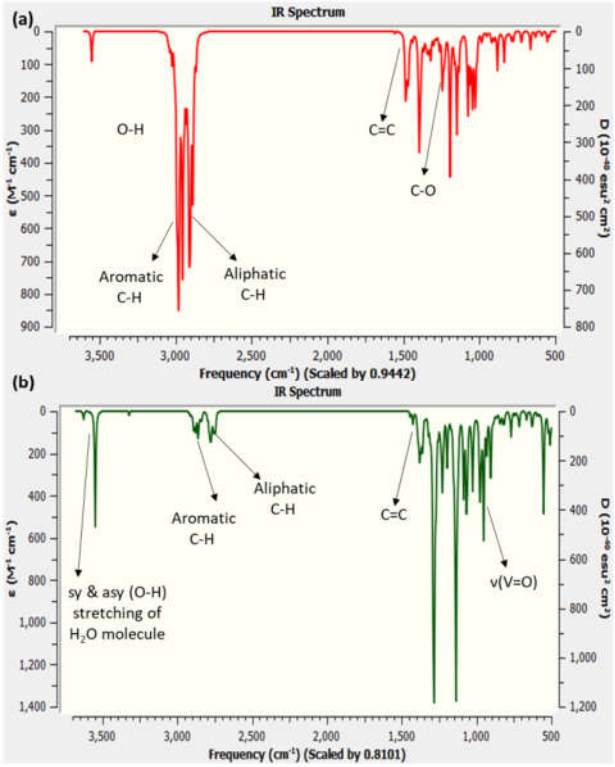

Figure 4. (a) Simulated (DFT) IR spectra of VitE only and (b) synthesized vanadyl(II) vitamin E complex (Vcom).

The spatial distribution of HOMO and LUMO orbitals, along with their energy gap (ΔE), for VitE and Vcom are visualized in Figure 5a and b. The ΔE values were calculated to be 4.7976 eV for VitE and 3.7998 eV for Vcom, indicating a lower energy barrier for electron excitation in Vcom, potentially enhancing its reactivity [37].

This energy gap correlates with the chemical stability of the molecules. Smaller energy gaps indicate higher chemical reactivity, lower kinetic stability, and a softer nature, whereas larger energy gaps suggest the opposite. Vcom's smaller energy gap suggests greater stability compared to VitE. The energy gap between these "electron zones" (HOMO and LUMO) acts like a gatekeeper. A smaller gap makes it easier for electrons to jump through, so the molecule is more reactive and less stable. Conversely, a larger gap makes it harder to jump, leading to a more stable and less reactive molecule. Interestingly, Vcom has a smaller gap than VitE. This tells us that Vcom, despite being a complex, is surprisingly more stable than the simpler VitE molecule. This is because its' wider "energy bridge" makes it less prone to chemical reactions and disruptions. Table 1 summarizes some key properties of these molecules, derived from the gas-phase analysis, HOMO-LUMO properties, and optimized geometries.

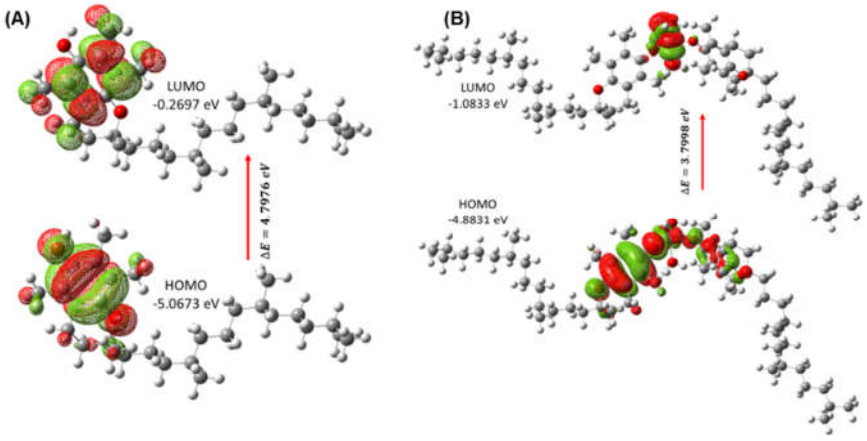

Figure 5. Spatial plot of HOMO and LUMO with their energy gap for VitE (a) and Vcom (b).

Table 1. Some key theoretical molecular characteristics of the VitE and Vcom.

Parameters	RB3LYP/ lanL2DZ	
	VitE	Vcom
Minimum SCF energy (a.u.)	-1285.372901	-2835.359883
Polarizability (α) (a.u.)	313.728988	438.428697
Dipole moment (Debye)	0.763794	4.466582
Zero point vibrational energy (kcal/mol)	467.36228	1035.14564
Total thermal energy (kcal/mol)	490.706	1070.000
Electronic spatial extent (a.u.)	34387.6834	171458.8491
Frontier MO energies (eV)		
LUMO	-0.2696	-1.0833
HOMO	-5.0673	-4.8831
HOMO-1	-5.9792	-5.1623
Gap (HOMO – LUMO)	4.7976	3.7998
Gap (HOMO-1 – LUMO)	5.7096	4.0790

Molecular docking studies

Molecular docking studies were performed to investigate the binding affinities of VitE and the synthesized Vcom complex with prepared Vitamin E receptors, α-TTP, and NF-κB. The most favorable binding poses were identified and compared theoretically. The results revealed a lower binding potential energy for Vcom compared to VitE for both receptors (Table 2).

Table 2. The docking score of VitE and synthesized complex docked with two receptors [α-TTP and NF-kB.

Ligand	Binding free energy (kcal/mol)	
	PDB ID: 1OIP	PDB ID: 1SVC
VitE	-10.8	-7.6
Vcom	-14.8	-11.2

When interacting with α-TTP, Vcom showed the highest docking energy value, with a theoretical binding energy of 14.8 kcal/mol. When compared to other interactions, the greater binding energy value of Vcom with α-TTP indicates a stronger connection. Table 3 offers further crucial information about docking analysis.

Table 3. The interactions of VitE and Vcom with α-TTP and NF-kB receptors.

Ligand+Receptor	Interactions	
	H-Bond	Others
VitE + α-TTP	Ser136	Phe133, Phe158, and Phe182 (π-Alkyl); and Val182 and Phe158 (π-Sigma)
Vcom + α-TTP	ser140, ser136, and Val182	Tyr117, Phe133, and Phe187 (π-Sigma); and Val191, Ala156 (π-Alkyl)
VitE + NF-kB	Lys218	Thymine11 (π-Sigma); Lys218 (π-Cation) and Thymine11, Cytosine14, Guanine7, Adenine9, Adenine10,and Lys218 (π-Alkyl)
Vcom + NF-kB	Gly31 and Guanine6	Guanine7, Glu198, and Asp217 (π-Anion); Thymine11, Guanine7, Adenine8, Adenine9, and His181 (π-Alkyl)

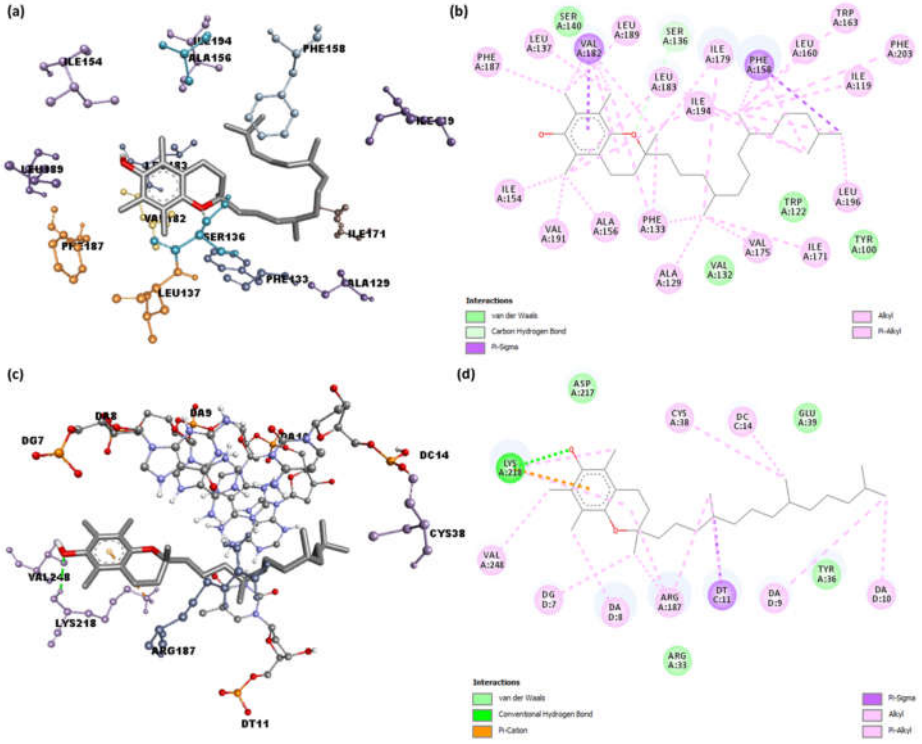

Figure 6. (a) The three-dimensional model and (b) two-dimensional model of the interactions for α-TTP receptor docked with VitE; (c) the three-dimensional model and (d) two-dimensional model of the interactions for α-TTP receptor docked with Vcom.

Figure 6 compares the interactions between VitE and Vcom with α-TTP. While both molecules form hydrogen bonds with Ser136 and Ser140, Vcom also engages with Tyr117, Phe133, and Phe187 in π-sigma interactions, and Val191 and Ala156 contribute to π-alkyl interactions. This suggests slightly different binding patterns for the two molecules.

Just like with α-TTP, VitE and the Vcom complex interact with specific amino acids on the protein NF-κB, including hydrogen bonds and different types of π interactions. VitE forms a hydrogen bond with Lys218. The π-Sigma interaction with Thymine11, π-Cation interaction with Lys218 and π-Alkyl with Thymine11, Cytosine14, Guanine7, Adenine9, Adenine10,and Lys21. On the other hand, Vcom with NF-κB for hydrogen bond with Gly31 and Guanine6, π-Anion interaction with Guanine7, Glu198, and Asp217, π-alkyl interaction with Thymine11, Guanine7, Adenine8, Adenine9, and His181. This suggests that Vcom might have a stronger overall binding affinity to both Vitamin E receptors, particularly with α-TTP where its interactions are wider.

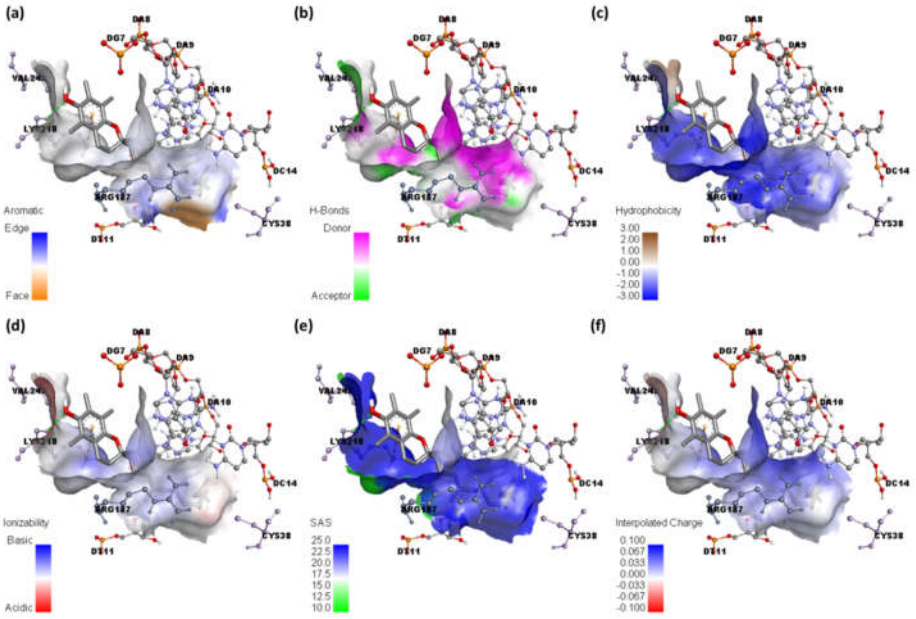

Figure 7. Illustration of the following surfaces: (a) solvent accessible; (b) hydrogen binding; (c) hydrophobic; (d) ionizability; (e) aromatic; and (f) interpolated charge; between α-TTP and Vcom.

Aromatic, hydrophobicity, hydrogen bond, SAS, interpolated charge, and ionizability surfaces study

Understanding how aromatic rings in molecules interact is crucial in many fields, such as drug design and protein function. Therefore, to understand how VitE and the Vcom complex interact with their protein "docking sites," we used a software called Discovery Studio (DS) to visualize different types of surfaces around these areas [38, 39]. Figure 7, show surfaces for things like hydrogen bonds, aromatic interactions, and solvent accessibility. This analysis can reveal important clues about how these molecules interact with other substances as well [40].

Figure 7, offer detailed visual representations of the docking site, focusing on aromatic surfaces and hydrogen bond interactions. The orange and blue colors depict the aromatic features of the molecule, while green and pink regions with connecting lines highlight the hydrogen bonds formed between specific amino acids and the molecule. This visual approach provides valuable insights into the binding pattern and the key amino acid players involved [41]. To understand how VitE interacts with its protein "docking site," we used different surface views in Figure 7. One view shows hydrophobic regions (blue) and hydrophilic regions (neutral or contrasting colors), which helps us see how the molecule interacts with water [42]. Another view shows the accessible surface area (blue) and less accessible areas (green), which tells us where other molecules might be able to connect with the protein [43]. Finally, an ionization view shows acidic (red) and basic (blue) areas, helping us understand the molecule's electrical properties [44]. In the case of VitE with α-TTP, none of the residues were identified as ionizable [45-48].

CONCLUSION

The association and characterization of synthesized complex between vanadyl(II) sulfate and vitamin E (Vcom) were delineated using spectral and analytical data. These findings indicate a square-pyramidal geometry for the resultant complex. The theoretical data obtained through DFT calculations has been instrumental in exploring the molecular geometry. Analyzing the band gap energies of both VitE and Vcom indicates that Vcom exhibits greater stability. These DFT derived molecular parameters provide valuable insights for future research. Molecular docking studies have shown that the synthesized Vcom interacts more efficiently with both Vitamin E receptors, α-tocopherol transfer protein (α-TTP) and nuclear factor kappa B (NF-κB), compared to VitE. Notably, Vcom demonstrates a stronger affinity for α-TTP, with the highest binding energy value. Surface binding studies also confirm the superior interaction of Vcom with these receptors when compared to VitE.

ACKNOWLEDGMENT

The authors extend their appreciation to the Deputyship for Research and Innovation, Ministry of Education in Saudi Arabia, for funding this research work through the project number WE-44-0289.

REFERENCES

1. Djordjevic, C.; Wampler, G.L. Antitumor activity and toxicity of peroxo heteroligand vanadates(V) in relation to biochemistry of vanadium. *J. Inorg. Biochem*. **1985**, 25, 51-55.
2. Sakurai, H.; Kojima, Y.; Yoshikawa, Y.; Kawabe, K.; Yasui, H. Antidiabetic vanadium(IV) and zinc(II) complexes. *Coord. Chem. Rev*. **2002**, 226, 187-198.
3. Bishayee, A.; Chatterjee, M. Inhibitory effect of vanadium on rat liver carcinogenesis initiated with diethylnitrosamine and promoted by phenobarbital. *Br. J. Cancer*. **1995**, 71, 1214-1220.
4. Chakraborty, A.; Chatterjee, M. Enhanced erythropoietin and suppression of gamma-glutamyl transpeptidase (GGT) activity in murine lymphoma following administration of vanadium. *Neoplamsa* **1994**, 41, 291-296.
5. Cuncic, C.; Desmarais, S.; Detich, N.; Tracey, A.S.; Gresser, M.J.; Ramachandran, C. Bis (N,N-dimethylhydroxamido) hydroxooxovanadate inhibition of protein tyrosine phosphatase activity in intact cells: comparison with vanadate. *Biochem. Parmacol*. **1999**, 58, 1859-1867.
6. D'Cruz, O.J.; Dong, Y.; Uckun, F.M. Apoptosis-inducing oxovanadium(IV) complexes of 1,10-phenanthroline against human ovarian cancer. *Anti-Cancer Drugs.* **2000**, 11, 849-858.
7. Evangelou, A.M. Vanadium in cancer treatment. *Crit. Rev. Oncol. Hematol*. **2002**, 42, 249-265.

8. Tsiani, E.; Fantus, I.G. Vanadium compounds: Biological actions and potential as pharmacological agents. *Trends Endocrinol. Metab*. **1997**, 8, 51-58.
9. McNeill, J.H.; Yuen, V.G.; Hoveyda, H.R.; Orvig, C. Bis (maltolato) oxovanadium(IV) is a potent insulin mimic. *J. Med. Chem*. **1992**, 35, 1489-1491.
10. Thompson, K.H.; Orvig, C. Coordination chemistry of vanadium in metallopharmaceutical candidate compounds. *Coord. Chem. Rev*. **2001**, 219, 1033-1053.
11. Orvig, C.; Thompson, K.H.; Battell, M.; McNeill, J.H. Vanadium compounds as insulin mimics. *Met. Ions Biol. Syst*. **1995**, 31, 575-594.
12. Thompson, K.H.; Orvig, C. Vanadium compounds in the treatment of diabetes. *Met. Ions Biol. Syst*. **2004**, 41, 221-252.
13. Cuncic, C.; Detich, N.; Ethier, D.; Tracey, A.S.; Gresser, M.J.; Ramachandran, C. Vanadate inhibition of protein tyrosine phosphatases in Jurkat cells: Modulation by redox state. *J. Biol. Inorg. Chem*. **1999**, 4, 354-359.
14. Schieven, G.L.; Wahl, A.F.; Myrdal, S.; Grosmaire, L.; Ledbetter, J.A. Lineage-specific induction of B cell apoptosis and altered signal transduction by the phosphotyrosine phosphatase inhibitor bis (maltolato) oxovanadium(IV). *J. Biol. Chem*. **1995**, 270, 20824-20831.
15. Krejsa, C.M.; Nadler, S.G.; Esselstyn, J.M.; Kavanagh, T.J.; Ledbetter, J.A.; Schieven, G.L. Role of oxidative stress in the action of vanadium phosphotyrosine phosphatase inhibitors: Redox independent activation of NF-κB. *J. Biol. Chem*. **1997**, 272, 11541-11549.
16. Thompson, K.H.; Tsukada, Y.; Xu, Z.; Battell, M.; McNeill, J.H.; Orvig, C. Influence of chelation and oxidation state on vanadium bioavailability, and their effects on tissue concentrations of zinc, copper, and iron. *Biol. Trace Elem. Res*. **2002**, 86, 31-44.
17. Thompson, K.H.; McNeill, J.H. Effect of vanadyl sulfate feeding on susceptibility to peroxidative change in diabetic rats. *Res. Commun. Chem. Pathol. Pharmacol*. **1993**, 80, 187-200.
18. Rychter, A.M.; Hryhorowicz, S.; Słomski, R.; Dobrowolska, A.; Krela-Kaźmierczak, I. Antioxidant effects of vitamin E and risk of cardiovascular disease in women with obesity–A narrative review. *Clin. Nutr.* **2022**, 41, 1557-1565.
19. Jiang, Q.; Im, S.; Wagner, J.G.; Hernandez, M.L.; Peden, D.B. Gamma-tocopherol, a major form of vitamin E in diets: Insights into antioxidant and anti-inflammatory effects, mechanisms, and roles in disease management. *Free Radic. Biol. Med.* **2022**, 178, 347-359.
20. Garcia, E.I.C.; Elghandour, M.M.; Khusro, A.; Alcala-Canto, Y.; Tirado-González, D.N.; Barbabosa-Pliego, A.; Salem, A.Z. Dietary supplements of vitamins E, C, and β-carotene to reduce oxidative stress in horses: An overview. *J. Equine Vet. Sci.* **2022**, 110, 103863-103885.
21. Li, X.Y.; Meng, L., Shen, L.; Ji, H.F. Regulation of gut microbiota by vitamin C, vitamin E and β-carotene. *Food Res. Int.* **2023**, 169, 112749-112764.
22. Refat, M.S.; El-Shazly, S.A. Identification of a new anti-diabetic agent by combining $VOSO_4$ and vitamin E in a single molecule: studies on its spectral, thermal and pharmacological properties. *Eur. J. Med. Chem.* **2010**, 45, 3070-3097.
23. Frisch, M.; Clemente, F. Gaussian 09, revision a. 01, mj frisch, gw trucks, hb schlegel, ge scuseria, ma robb, jr cheeseman, g. Scalmani, V. Barone, B. Mennucci, GA Petersson, H. Nakatsuji, M. Caricato, X. Li, HP Hratchian, AF Izmaylov, J. Bloino, G. Zhe, **2009**, 20-44.
24. Jakubikova, E.; Rappé, A.K.; Bernstein, E.R. Density functional theory study of small vanadium oxide clusters. *J. Phys. Chem. A* **2007**, 111, 12938-12943.
25. Hariharan, P.C.; Pople, J.A. The effect of d-functions on molecular orbital energies for hydrocarbons. *Chem. Phys. Lett.* **1972**, 16, 217-219.
26. Zhurko G.A.; Zhurko D.A. Chemcraft - graphical program for visualization of quantum chemistry computations. Ivanovo, Russia, Academic version 1.5. **2004**.
27. O'Boyle, N.M.; Banck, M.; James, C.A.; Morley, C.; Vandermeersch, T.; Hutchison, G.R. Open babel: An open chemical toolbox. *J. Cheminformatics* **2011**, 3, 33-47.

28. Dallakyan, S. PyRx-python prescription v. 0.8 .*The Scripps Research Institute*, **2008,** 2010.
29. Chu, C.-H.; Li, K.-M.; Lin, S.-W.; Chang, M.D.-T.; Jiang, T.-Y.; Sun, Y.-J. Crystal structures of starch binding domain from *Rhizopus oryzae* glucoamylase in complex with isomaltooligosaccharide: Insights into polysaccharide binding mechanism of CBM21 family. *Proteins: Struct. Funct. Bioinfor.* **2014**, 82, 1079-1085.
30. Rehman, M.T.; AlAjmi, M.F.; Hussain, A. Natural compounds as inhibitors of SARS-CoV-2 main protease (3CLpro): A molecular docking and simulation approach to combat COVID-19. *Cur. Pharm. Desi.* **2021**, 27, 3577-3589.
31. Eberhardt, J.; Santos-Martins, D.; Tillack, A.F.; Forli, S. AutoDock Vina 1.2.0: New docking methods, expanded force field, and python bindings. *J. Chem. Inf. Model* **2021**, 61, 3891-3898.
32. Shakya, S.; Khan, I.M.; Ahmad, M. Charge transfer complex based real-time colorimetric chemosensor for rapid recognition of dinitrobenzene and discriminative detection of Fe^{2+} ions in aqueous media and human hemoglobin. *J. Photochem. Photobio. A: Chem.* **2020**, 392, 112402-112415.
33. Islam, M.R.; Shakya, S.; Selim, A.; Alam, M.S.; Ali, M. Solvatochromic absorbance and fluorescence probe behavior within ionic liquid + γ-butyrolactone mixture. *J. Chem. Eng. Data* **2019**, 64, 4169-4180.
34. Yu, W.; He, X.; Vanommeslaeghe, K.; MacKerell, A.D., Jr. Extension of the CHARMM general force field to sulfonylcontaining compounds and its utility in biomolecular simulations. *J. Comput. Chem.* **2012**, 33, 2451-2468.
35. Foresman, J.B. in Frisch, E. (Ed.), *Exploring Chemistry with Electronic Structure Methods: A Guide to Using Gaussian*, Gaussian Inc.: Pittsburg, PA; **1996**.
36. Murugavel, S.; Ravikumar, C.; Jaabil, G.; Alagusundaram, P. Synthesis, crystal structure analysis, spectral investigations (NMR, FT-IR, UV), DFT calculations, ADMET studies, molecular docking and anticancer activity of 2-(1-benzyl-5-methyl-1H-1, 2, 3-triazol-4-yl)-4-(2-chlorophenyl)-6-methoxypyridine–a novel potent human topoisomerase IIα inhibitor. *J. Mol. Struct.* **2019**, 1176, 729-742.
37. Khan, I.M.; Shakya, S. Exploring colorimetric real-time sensing behavior of a newly designed CT complex toward nitrobenzene and Co^{2+}: Spectrophotometric, DFT/TD-DFT, and mechanistic insights. *ACS Omega* **2019**, 4, 9983-9995.
38. Akram, M.; Lal, H.; Shakya, S.; Kabir-ud-Din. Multispectroscopic and computational analysis insight into the interaction of cationic diester-bonded gemini surfactants with serine protease α-chymotrypsin. *ACS Omega* **2020**, 5, 3624-3637.
39. Khan, I.M.; Shakya, S.; Islam, M.; Khan, S.; Najnin, H. Synthesis and spectrophotometric studies of CT complex between 1,2-dimethylimidazole and picric acid in different polar solvents: exploring antimicrobial activities and molecular (DNA) docking. *Phys. Chem. Liq.* **2021**, 59, 753-769.
40. Alamri, A.S.; Alhomrani, M.; Alsanie, W.F.; Alyami, H.; Shakya, S.; Habeeballah, H.; Alamri, A.; Alzahrani, O.; Alzahrani, A.S.; Alkhatabi, H.A.; Felimban, R.I. Enhancement of haloperidol binding affinity to dopamine receptor via forming a charge-transfer complex with picric acid and 7,7,8,8-tetracyanoquinodimethane for improvement of the antipsychotic efficacy. *Molecules* **2022**, 27, 3295-3308.
41. Alsanie, W.F.; Alamri, A.S.; Alyami, H.; Alhomrani, M.; Shakya, S.; Habeeballah, H.; Alkhatabi, H.A.; Felimban, R.I.; Alzahrani, A.S.; Alhabeeb, A.A.; Raafat, B.M. Increasing the efficacy of seproxetine as an antidepressant using charge–transfer complexes. *Molecules* **2022**, 27, 3290-3310.
42. Ranjbar, A.; Jamshidi, M.; Torabi, S. Molecular modelling of the antiviral action of Resveratrol derivatives against the activity of two novel SARS CoV-2 and 2019-nCoV receptors. *Eur. Rev. Med. Pharmacol. Sci*. **2020**, 24, 7834-7844.

43. Hussen, N.H.; Hasan, A.H.; Jamalis, J.; Shakya, S.; Chander, S.; Kharkwal, H.; Murugesan, S.; Bastikar, V.A.; Gupta, P.P. Potential inhibitory activity of phytoconstituents against black fungus: In silico ADMET, molecular docking and MD simulation studies. *Comput. Toxicol*. **2022**, 24, 100247-100261.
44. Ranjbar, A.; Jamshidi, M.; Torabi, S. Molecular modelling of the antiviral action of Resveratrol derivatives against the activity of two novel SARS CoV-2 and 2019-nCoV receptors. *Eur. Rev. Med. Pharmacol. Sci*. **2020**, 24, 7834.
45. Khan, M.S.; Khalid, M.; Ahmad, M.S.; Kamal, S.; Shahid, M.; Ahmad, M.; Effect of structural variation on enzymatic activity in tetranuclear (Cu4) clusters with defective cubane core. *J. Biomole. Struct. Dynam.* **2022**, 40, 9067-9080.
46. Khan, M.S.; Ansari, M.A.H.; Khalid, M.; Shahid, M.; Ahmad, M. Synthesis, characterization, single-crystal X-ray study and sensing properties of a designed dinuclear Cu(II) system. *Inorg. Nano-Metal Chem.* **2023**, 1-8. (DOI: 10.1080/24701556.2023.2188454)
47. Khan, M.S.; Leong, Z.Y.; Li, D.S.; Qiu, J.; Xu, X.; Yang, H.Y. A mini review on metal-organic framework-based electrode materials for capacitive deionization. *Nanoscale* **2023**, 15, 15929-15949.
48. Khan, M.S.; Li, Y.; Yang, L.; Yan, Z.C.; Li, D.S.; Qiu, J.; Xu, X.; Yang, H.Y. Improving capacitive deionization performance through tailored iodine-loaded ZIF-8 composites. *Desalination* **2024**, 117486-117497.